Status and prospects for the KLOE-2 experiment

2011 J. Phys.: Conf. Ser. 335 012070

(http://iopscience.iop.org/1742-6596/335/1/012070)

Journal of Physics: Conference Series **335** (2011) 012070 doi:10.1088/1742-6596/335/1/012070

Status and prospects for the KLOE-2 experiment

Stefano Miscetti
on behalf of the KLOE-2 collaboration

Laboratori Nazionali di Frascati dell'INFN, via Enrico Fermi 40, I-00044 Frascati (Rome) Italy

E-mail: stefano.miscetti@lnf.infn.it

Abstract. The KLOE-2 experiment is starting a data taking campaign at DAϕNE, the e^+e^- collider of the Frascati Laboratories of INFN, with the aim of integrating O(20 fb^{-1}) in few years of running. The KLOE-2 detector has been upgraded with the insertion of small angle taggers for $\gamma\gamma$ physics. The construction of larger upgrades such as an Inner Tracker and two small angle calorimeters is underway.

1. From KLOE to KLOE-2

The KLOE experiment is starting a new data taking campaign (as KLOE-2) at DAϕNE, the e^+e^- collider of the Frascati Laboratories of INFN. The machine has been recently modified by using a Crabbed Waist scheme [1] in the interaction region. An increase of $\sim$ a factor of 3 in luminosity is expected to get O(20 fb^{-1}) in few years of running. The KLOE-2 [2] detector has also been upgraded with the insertion of small angle taggers for $\gamma\gamma$ physics. An integrated luminosity of 5 fb^{-1} should be collected in the first year of running, phase-1. The construction of larger upgrades (see Fig. 1): an Inner Tracker, IT, and two small angle calorimeters is underway with the aim of completing their insertion at the beginning of 2012, phase-2.

The KLOE-2 roll-in in DAϕNE was succesfully completed in January 2010 while the insertion of the new IP region, surrounded by our background screens, was done in June 2010. The KLOE magnet was cooled down in June and turned on at the nominal value of 5.2 kGauss for a month in July. This allowed us to perform all final calibrations for the calorimeter, EMC, and the tracking, DCH, systems. After the August shutdown, we got troubles in cooling the magnet which needed to be warmed up to room temperature before succeeding to reach a stable cool down. In November, first beams with normal optics were circulating in DAϕNE. Currents up to 1 A were reached both for the e^- and e^+ beams and many improvements found (vertical beam dimension down to 150 μm achieved). First collisions were tried at low currents (up to 300 mA/beam) without turning on the Crab sextupoles and delivering instantaneous luminosity of few 10^{31} cm^{-2}sec^{-1}. However the machine background in the detector was too high to collect data in a reasonable way. On January 2011, the septum magnet for the e^+ injection line accidentaly broke and we keep running e^- beam for few weeks to improve the background conditions. Apart few changes in the optics, we succeeded to run with 700 mA of electrons with all detector "on" after having hardened the tripping condition of the DCH. The machine background was not yet optimal since we got $\sim$ 10 MHz of single EMC clusters due to machine background. In February, we made a 5 days access on the KLOE-2 detector to add some additional lead screens (1 cm thick) and a special lead plug around the inner quadrupoles area.

At the moment of writing, we have completed our fixing and a new septum magnet has been inserted. We expect to start the run in the next weeks.

2. The physics program

The KLOE-2 physics program is very wide and aims to improve the experimental studies on hadronic physics at low energy, kaons, $\gamma\gamma$ physics, the contribution of hadron vacuum polarization to the muon anomalous magnet, CKM unitarity and Lepton Universality, CPT symmetry and quantum interferometry, QI, studies. A full description of this program can be found elsewhere [3]. Detailed analysis of QI studies and searches for a "U" boson from a dark gauge sector were presented at this meeting and can be found in the same proceedings [4, 5]. The relevance of $\gamma\gamma$ physics is reported in section 3 where we describe also the implication of the new tagger system. Regarding the quantum interferometry, we recall only that, in the phase-2 of the experiment, the presence of the IT will improve by a factor between 3 to 4 the vertex resolution and consequently the reconstruction of the relevant QI parameters. As an example, assuming that the K_S, K_L pair decays to the same final state $\pi^+\pi^-$, the distribution of $\Delta T = |t1-t2|$, where t1 and t2 are the decay times of the K_S-K_L, shows a deep around zero since no simultaneous decays can occur due to destructive quantum interference. The reconstruction of the deep gets better increasing the vertex resolution reaching almost an "ideal" curve with the insertion of the IT in the tracking. This resolution improvement acts on the determination of the QI parameters as a fourfold increase on luminosity.

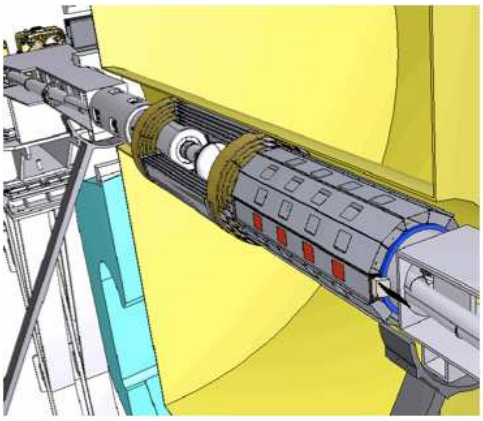

Figure 1. Expanded view of the inner KLOE-2 region. The IT and QCALT detectors are shown close to the IP.

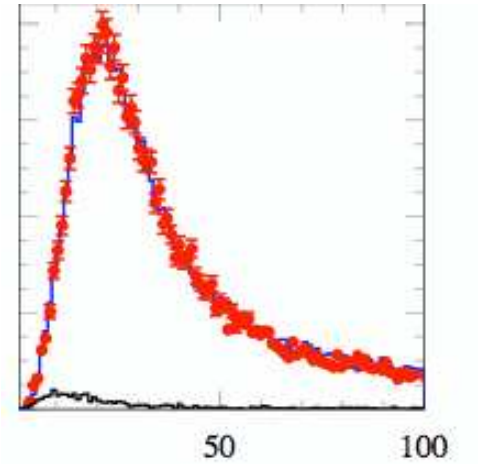

Figure 2. Distribution of χ^2 for events with six photons and a K_L-crash. Red points (data), blue line (MC bkg), black line (MC signal).

In this section, we describe in detail only two analysis examples which can be carried out with the first 5 fb^{-1}: the search for $\phi \to KK\gamma$ and $K_S \to 3\pi^0$ decay chains.

The $\phi \to K\bar{K}\gamma$ process should proceed through the $\phi \to [a_0(980) + f_0(980)]\gamma$ intermediate state. In KLOE, we searched for this channel by looking at the decay chain $\phi \to K_S K_S \gamma \to \pi^+\pi^-\pi^+\pi^-\gamma$. The main backgrounds being the resonant $e^+e^- \to \phi\gamma \to K_S K_L$ with an IRS photon and the continuum $e^+e^- \to \pi^+\pi^-\pi^+\pi^-\gamma$ processes. From an integrated luminosity of 2.2 fb^{-1}, 5 candidates are found in data, while 3.2 ± 0.7 background events are expected from MC . This leads to BR($\phi \to K\bar{K}\gamma$) $< 1.9 \times 10^{-8}$ at 90% CL. Scaling these numbers to the KLOE-2 statistics a sensitivity of $BR(\phi \to K^0\bar{K}^0\gamma) < 1 \times 10^{-8}$ is expected.

The best limit on the CP–violating decay $K_S \to 3\pi^0$ comes from the analysis of ~ 450 pb^{-1} collisions taken during 2001-2002. In this search, we tagged the K_S by means of a K_L interaction in the calorimeter, K_L-crash, and looked for events with six prompt photons. Discriminating variables based on kinematic fit and photon pairing were used to elimate the obvious background of $K_S \to 2\pi^0 + 2$ additional photons. We got 2 candidates with an expected background of 3.13 $\pm$ 0.82 events and a reconstruction efficiency of 24.4 %. We set the limits to be 1.2×10^{-7} at 90 % C.L.

We have lately started a production campain with a larger sample (1.7 fb^{-1} data, 3.4 fb^{-1} MC) aiming to a much stronger background reduction. Driven by MC studies of signal and background, we add two cuts: (i) splitting recovery, by cutting on the minimal 3-D distance between clusters, R_{min}, and (ii) fake-rejection, by hardening the K_L-crash selection (E > 150 MeV and $0.200 < \beta_K < 0.225$). In Fig. 2, we show a good data/MC agreement in the χ^2 distribution of the kinematic fit for the six photon sample. The new cuts show their rejection power in MC. At the end of a preliminary optimization, we find 0 candidates in the simulated sample while keeping a reasonable overall efficiency of ~ 22 %. We expect to reach a limit which is not anymore background limited and so will scale with increasing luminosity at values of ~ 3 (1) $\times 10^{-8}$ for the KLOE (2.5 fb^{-1}) or KLOE-2 phase-1 (5 fb^{-1}) data sets. The addition of the upgrades and a larger data set will lead to observe for the first time such a decay.

3. $\gamma\gamma$ physics and status of the $\gamma\gamma$ taggers

The $e^+e^- \to e^+e^-\gamma^*\gamma^* \to e^+e^-X$ process, where X is the final state resulting from the fusion of two photons, gives access to states with $J^{PC} = 0^{\pm+}$, $2^{\pm+}$. In the low-energy region covered by the KLOE detector, $m_{\pi^0} < W_{\gamma\gamma} < 700$ MeV, existing measurements are affected by large statistical and systematic uncertainties. At KLOE, where there is no tagging of the outgoing e^+e^-, $\gamma\gamma$ interactions have been studied using 240 pb^{-1} collected at $\sqrt{s} = 1$ GeV, as the main source of background comes from ϕ decays. We started looking for the $e^+e^- \to e^+e^-\pi^0\pi^0$ process. A large excess with respect to known background is evident at low $M_{4\gamma}$ values. The η radiative width,$\Gamma_{\eta\gamma\gamma}$, is usually extracted from the measurement of the $e^+e^- \to e^+e^-\eta$ cross section. The KLOE analysis is performed using the $\eta \to \pi^+\pi^-\pi^0$ decay channel. After background rejection, distributions of longitudinal momentum (p_L) and recoil missing mass (M^2_{miss}) are independently fitted with the superposition of MC shapes for signal and background More than 600 $e^+e^- \to e^+e^-\eta \to e^+e^-\pi^+\pi^-\pi^0$ events are obtained.

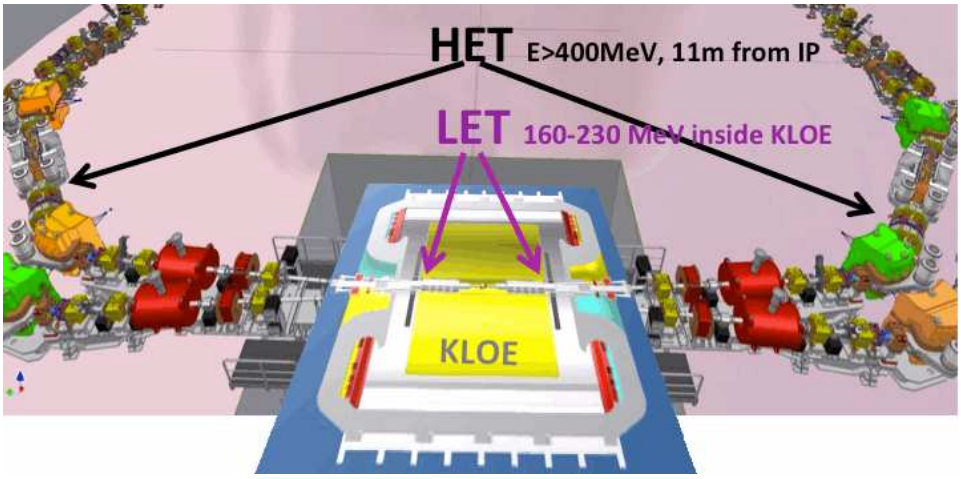

Figure 3. Scheme of the $\gamma\gamma$ taggers in DAΦNE and KLOE.

These KLOE analyses represent also a feasibility test for the study of $\gamma\gamma$ processes in KLOE-

2, that will take advantage of a tagging system for the detection of scattered e^+/e^- in the final state thus allowing to perform these measurements also at the ϕ peak. Moreover, with the tagger, it would be possible to measure the transition form factors $\mathcal{F}_{X\gamma^*\gamma^*}(q_1^2, q_2^2)$ as a function of the momentum of the virtual photons, q_1^2 and q_2^2, relevant for the evaluation of the hadronic light-by-light contribution to the muon magnetic anomaly. The installation of $\gamma\gamma$ taggers [6] is almost completed. In Fig. 3, the taggers system is shown. It consists of a low energy tagger, LET, inside KLOE and a high energy tagger, HET, after the first bending magnet 11 m far away from the IP. In year 2010 the detectors have been realized and the LET calorimeters have been installed on the final focusing region of DAϕNE. The LET is composed by two stations of 20 LYSO crystals, each readout by 3×3 mm^2 SIPM's from Hamamatsu. The expected energy resolution is of ~ 7 % at 100 MeV. All channels have been acquired by the KLOE DAQ system and test with Cosmic rays are in progress. The HET consists instead of two stations of position detectors composed of 32 scintillator counters of $5 \times 6 \times 3$ mm^3 readout by small size PMTs. The HET optical system is ready, including shaped optical guides and scintillators wrapped with aluminized mylar. The three main components of the HET mechanics are the insertion and vacuum systems, the structural support for the phototubes and the external support. The insertion and vacuum systems have been installed inside the beam pipe. The structural support for the phototubes and the external support have been designed and are under construction. Two out of four boards for the acquisition chain, i.e., the Front End Buffer board (FEBb), and the Fast Discriminator Shaper board (FDSb), are being tested, while the others, i.e. the Acquisition V5 board (ACQ-V5b) and the Slow Environment Control System board (SECSb), are being constructed.

4. The Inner Tracker

The Inner Tracker[7] (IT) is composed by four cylindrical layers of triple-GEM (CGEM) at radii from 13 to 23 cm, and, as shown in Fig. 1, will get installed between the spherical beam pipe and the drift chamber. The total active length for all layers is 70 cm. The anode readout of each CGEM is segmented with 650–μm–pitch, XV–patterned strips at a stereo angle of $\sim 40°$, for a total of 30,000 FEE channels based on GASTONE ASIC [8], a dedicated 64–channels chip developed for the KLOE-2 experiment.

The construction and extensive test of a full-size CGEM prototype has demonstrated the feasibility of such a novel low–mass and dead–zone–free vertex detector. The final readout configuration has been successfully validated testing small planar prototypes operated in magnetic field. During 2010, to conclude the R&D phase, a large area planar GEM prototype of 300×700 mm^2 area has been built. This detector has been equipped with the GASTONE 64–channels final release, readout by the Off Gastone Electronic (OGE) board and tested at CERN-PS T9 beam-line in October, 2010.

The detector mechanics, assembly and quality control tools have been prepared and are now ready for the construction of the Inner Tracker. The Vertical Insertion System (VIS) has been built. This system will be used to assembly each IT layer by inserting the cylindrical electrodes one inside the other with high precision. In 2010 the activity has been mainly focused on the design of the detector components and tools necessary for the construction of the Inner Tracker: (i) **Detector Components**, the design of the detector components and construction tools originates from previous construction experience and, more specifically, for the construction of the full scale prototype of the CGEM [9]. In particular, the materials used for the CGEM were largely tested and validated for high-rate environments and for different gas mixtures (Ar, i-C4H10, CF4, CO2). The CGEM has the typical triple-structure of such a kind of micro-pattern gas detector: the gaps among the different electrodes of the detector (cathode-G1,G1-G2,G2-G3 and G3-anode) define the various regions of the detector itself: drift (3 mm wide), transfers and induction (2 mm wide). The frames are realized in EPCG203 fiberglass, a composite material

Figure 4. (Top) the aluminum moulds used for the construction of the cylindical electrodes, (bottom) Visual Inspection tool.

Figure 5. The assembly machine (VIS) used for the insertion of the electrodes one inside the other.

that allows precise machining, and are glued at the edge of the cylindrical electrodes outside their active area, define the various gaps of the detector. The most relevant modification with respect to the prototype design is represented by the embedded-anode, consisting of a very light honeycombed carbon fiber cylinder (CFC) on which the anode readout circuit is glued. The CFC acts as a rigid support for the whole detector layer. The 700 mm long GEMs are realized with the new single mask procedure that allows large area foils to be built[10]. In order to overcome the limit on the width of the raw material used for the GEM foils (600 mm), all the large electrodes of each layer are realized by splicing three smaller foils. The GEM foils, as well as the XV strip-pad patterned anode readout circuits and the cathode foils, are realized on the basis of our design by the CERN EST-DEM Printed Circuit Board Workshop.
(ii) **Construction and tooling**, the construction of the CGEM layers composing the IT are the same used for the prototype. The main construction steps can be summarized as follows: 1. the three GEMs, as well as the anode and cathode foils are glued together in order to obtain a single large foil. For this operation we exploit a precise Alcoa plane and a vacuum bag technique. 2. the large foil is then rolled on a very precise aluminum cylindrical mould covered with a 0.4 mm machined Teflon film for easy and safe extraction of the cylindrical electrode (fig. 4-top.left). The mould is then enveloped with the vacuum bag, and vacuum is applied for the glue curing time (about 12 hours). 3. the final assembling of a CGEM layer is performed by means of the Vertical Insertion System (VIS), fig. 5-right, a quite complex device that allows a precise and safe insertion of the cylindrical electrodes one inside the other.
(iii)**Material preparation and Quality Controls**, before the final assembly of the different detector parts, each component follows a well defined preparation procedure that generally includes a global optical inspection (see Fig. 4.bottom-left), a cleaning and an HV test. In

particular for GEMs the HV test is repeated at each construction step, in order to avoid the assembly of damaged GEM and to minimize the losses of precious components.
(iv)**Final readout**, the IT will be inserted between the beam pipe and the Drift Chamber inner wall. This location has very poor heat-exchange capability, it is not accessible after system installation and there is a reduced space for routing the cables. In addition, due to the GEM moderate gas gain, the front-end electronics must be installed on the detector to maximize S/N ratio. Therefore low power consumption and low number of connections are required together with high reliability of the entire system. To fulfill these requirements the GASTONE chip has been developed. This chip, built with the 0.35 CMOS technology, implements a mixed analog-digital circuit with 64 channels. Each channel is made of 4 blocks: a charge preamplifier with a sensitivity of about 20 mV/fC, a shaper, a leading-edge discriminator with programmable threshold and a monostable circuit to stretch the discriminated signals then allowing their synchronization with the KLOE trigger. Up to 180 chips assembled on 90 boards are required to fully instrument the detector. Digital output signals are serially readout by means of dedicated boards (then minimizing I/O cables) located about 4 m from the detector. Readout boards provide also LV and L0 to the front-end boards and ECS connection.

We have now the material to build two layers and we are proceeding with the construction of the cathods. We are still waiting the completion of the cleaning room to start assembly the layers which is foreseen to start in spring 2011.

5. The QCALT: a Quadrupole Calorimeter with Tiles

To increase the photon detection efficiency for $K_L \to 3\pi^0$ events we are developing a new Quadrupole Calorimeter to cover the area where the inner focalizing quadrupoles are located. There will be [11] two detectors, one per side with respect to the IP, named QCALT, (see Fig. 6), each one consisting of a dodecagonal structure, $\sim$ 0.9 m long, composed by a sampling of five layers of 5 mm thick scintillator plates alternated with 3.5 mm thick W/Cu (90/10) plates. The total absorption depth will be of 4.75 cm (5.5 X_0). The active part of each plane is divided into sixteen tiles of $\sim$5$\times$5 cm^2 area with 1 mm diameter WLS fibers embedded in circular grooves. Each fiber is then optically connected to a silicon photomultiplier of 1 mm^2 area, SiPM, for 80 channels/module and 1920 channels in total. The "T" in QCALT stays for tile, since we will read-out each tile singularly to get O(2 cm) resolution along z and be able to substain large rates O(MHz/module) thanks to the high granularity. Relying to the new quality SIPM of Hamamatsu, we have reached [12] a light yield of $\sim$ 30 p.e/MIP and a time resolution of $\sim$ 1 ns enough to obtain a reconstruction efficiency above 95% for photons with energy $>$ 20 MeV.

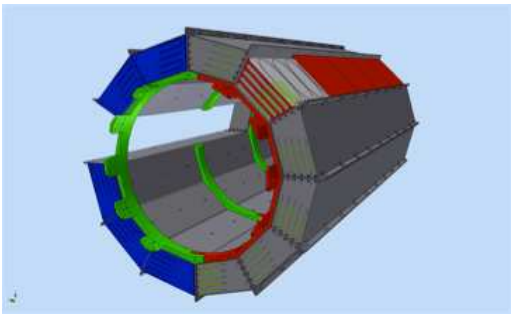

Figure 6. CAD drawings of the QCALT calorimeter.

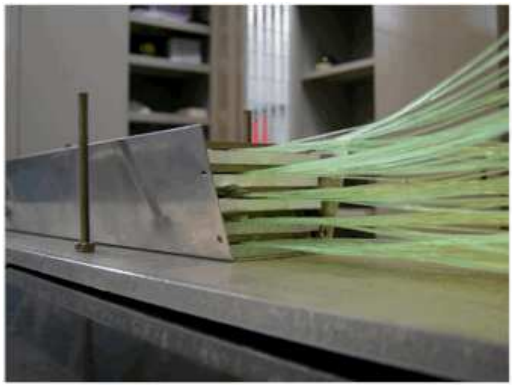

Figure 7. Picture of the QCALT module-0.

During 2010, we have realized the first full size "module-0", (see Fig. 7), in order to understand

the assembly techniques and the problems of integrating the readout in the reduced space available inside KLOE. During this construction we have learnt: (i) to survey the plastic scintillator thickness and how to prepare the grooves; (ii) to get well machined W/Cu plates; (iii) to "wrap" the tiles, easyness of construction and uniformity indicates that the best method to follow is to spray the tile with reflective paint; (iv) to couple fibers to SIPM's, a first set of fiber-SIPM PVC connector has been realized to check the optical contact reproducibility. We discovered that the mechanical precision in positioning should be better than 0.1 mm. To improve on this, we need for each module, to position the fibers in a PVC holder and match them with a PCB where 80 SIPM's will be bond; (v) to calibrate after assembly, this has been done acquiring cosmic rays,CR, in most of the columns (i.e. five planes at a time) by triggering with an external scintillator; (vi) to test the FEE; a set of twenty single channel amplifiers (dimension 10×20 mm^2) has been produced together with an HV driver done in NIM standard.

We have also studied the long-term stability of the tiles by firing a reference tile with a UV LED in a temperature controlled environment. We observed no hints of signal deterioration along an observation period of few months. We have then carried out a complete study on how to safely handle the calorimeter both during assembly and installation over the beam pipe support. During assembly, we will leave the fibers passing through the fiber holder and connect them to reference SIPM's by means of a special aluminum connector. This will allow to check the construction of each plane by firing with a UV LED along the different tiles. We plan to assembly one plane/day, one module/week for each assembly station. We will then bring the module to the SPCM of LNF for final fiber milling over the PVC holder.

Due to the difficulty of positioning 80 SIPM's in the front calorimeter face, we are working to integrate them over a PCB. First PCB prototypes have been realized and the IRST/FBK firm of Trento has built for us the first 160 SMD SIPMs of 1.2×1.2 mm^2 dimension to minimize the problem of alignment to the fiber. The IRST will also bond the SIPM's on the PCB. We expect to have a final working PCB for spring 2011.

The FEE, on detector, will consists of four boards/module of 20 channels/each where the preamplifiers and the HV regulator will be located. The OFF-detector electronics will consist of a 40 channel transition board that will do both the discrimination and the HV control. The readout will be organized by a TDC multihit with a range between 0.6 – 0.8 μsec and 1 ns resolution. Design of the final FEE boards is underway. We expect to have the first prototypes ready for spring 2011. At the end of 2010, we have ordered the material to start constructing the first six modules. We expect to start construction on spring 2011.

6. The CCALT: a Crystal Calorimeter with Timing

The CCALT is a crystal calorimeter which covers the solid angle between 10 and 18 degrees in order to extend our acceptance to low energy photons. The necessity of a calorimeter with high photon reconstruction efficiency (ϵ_γ >99% for $E_\gamma > 20$ MeV) and good time resolution (σ_t 200-500 ps) in this angular region has been proposed [11] with the double task of (i) vetoing the presence of unwanted photons in rare η and K_S channels ($K_S \to 2\gamma$ or $\eta \to \pi^0\gamma\gamma$) (ii) increasing the acceptance for very rare decays such as $K_S \to 3\pi^0$.

A good timing resolution and a fast response, ($\tau_{scint} < 50$ ns), are needed since the CCALT will be positioned (see Fig. 8) in between the interaction point and the first inner quadrupole, QD0, where an intense flux of photons of O(MHz)/side, produced from Tousheck particle, is expected. The detector is composed by two calorimeters, one per side with respect to the IP, each subdivided in twelve modules. Each module is constituted by four crystals of special trapezoidal shape with ~ 9 cm length and a transversal area of $\sim 25\times25$ mm^2 for the largest face. Given the reduced space available, we need fast and high density crystals with a large light yield. The crystal matching these requirements is the LYSO which has a density of 7.5 g/cm^3, a X_0 of 0.9 cm, a τ of 40 ns and a light yield of 500 p.e./ MeV when readout by a Bialcali PM. In 2009, we

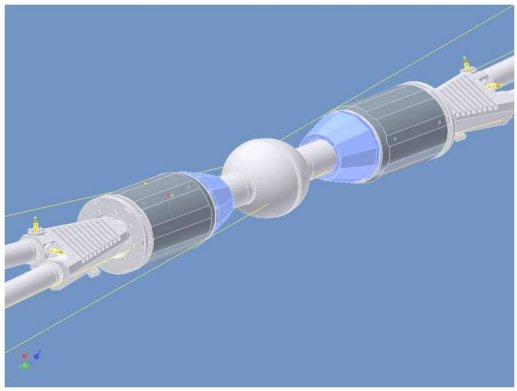

Figure 8. CAD drawings of the CCALT calorimeters (in blue) positioned over the IR.

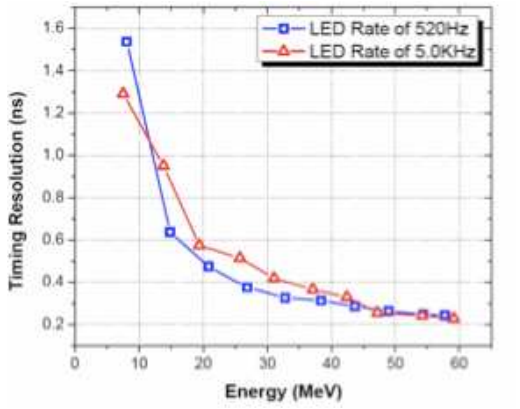

Figure 9. Dependence of the timing resolution of LYSO readout by SIPM's as a function of energy.

have built a first prototype done by an inner matrix of ten LYSO crystals readout by means of 5×5 mm^2 APD's. We have tested this prototype with 100 to 500 MeV electrons at the Beam Test Facility (BTF) [13] of LNF obtaining an energy resolution of 5% (13%) at 500 (100) MeV and a timing resolution between 100 to 200 ps. The energy resolution term proportional to 1/E resulted too large with respect to the measured noise term of 500 keV/channel. In order to understand that, we have constructed a better prototype readout by larger area APD's (10×10 mm^2) achieving a noise term of 150 keV/channel in laboratory tests. We plan to study the components of the energy resolution at the tagged photon beam facility of Mainz Microtron (MAMI) in spring 2011.

The integration with the other detectors, IT and QCALT, asks for tight requirements such as reducing as much as possible the thermal dissipation while respecting the space constraints. We have therefore investigated if we can succesfully readout the CCALT by means of large area SIPM's thus avoiding the usage of preamplifiers which have a typical power consumption of 100 mV/channel and a minimal transverse area of 10×20 mm^2. Two crystals have been optically connected with optical grease to two different SIPM's, a 4×4 (6×6) mm^2 from IRST/FBK (Hamamatsu) and their response to a UV LED has been tested both in charge and in time. In Fig. 9, we report the timing resolution of the crystal readout by IRST SIPM'a as a function of the energy for low rate pulsing. We see no deterioration of the timing response up to 50 kHz and a worsening up to a factor of 2 for rate close to the MHz. The timing resolution remains between 200 to 450 ps also at low energies, ($E_\gamma > 50$ MeV), showing that this technique will not be worse than a factor of two with respect to the APD readout.

References

[1] C. Milardi *et al.*, ICFA Beam Dyn. Newslett. 48 (2009) 23.
[2] http://www.lnf.infn.it/lnfadmin/direzione/KLOE2-LoI.pdf.
[3] G. Amelino-Camelia *et al.*, Eur. Phys. J. C 68 (2010) 619
[4] A. DeSantis "Status and prospects for Lorents and CPT violation tests at KLOE and KLOE-2 ", on these proceedings.
[5] S. Giovannella "U boson searches at KLOE-2 ", on these proceedings.
[6] D. Babusci *et al.*, arXiv:0906.0875 and LNF-10/17(P) INFN-LNF, Frascati, 2009.
[7] F. Archilli et al., arXiv:1002.2572v1 and LNF-10/3(P) INFN-LNF, Frascati,2010.
[8] A. Balla et al., Nucl. Inst. & Meth. **A 604** (2009) 23.
[9] G. Bencivenni et al., NSS Conference Record, 2007 IEEE, Volume 6 pp. 4666-4670.
[10] M. Alfonsi et al., Nucl. Inst. & Meth. **A 617** (2010) 151.

[11] F. Bossi et al., LNF-07/19(IR) INFN-LNF, Frascati, 2007.
[12] M. Cordelli et al., Nucl. Inst. & Meth. **A 617** (2010) 105.
[13] M. Cordelli et al., Nucl. Inst. & Meth. **A 617** (2010) 109.